


Cite this: *RSC Adv.*, 2020, 10, 39822

# Development of starch based intelligent films by incorporating anthocyanins of butterfly pea flower and TiO<sub>2</sub> and their applicability as freshness sensors for prawns during storage

Siji K. Mary,<sup>ab</sup> Rekha Rose Koshy,<sup>ab</sup> Jomol Daniel,<sup>a</sup> Jijo Thomas Koshy,<sup>a</sup> Laly A. Pothen<sup>ib</sup>\*<sup>b</sup> and Sabu Thomas<sup>ib</sup><sup>c</sup>

Intelligent pH sensitive starch films were developed by incorporation of anthocyanin pigment extracted from butterfly pea flower (BPE) and nanosized TiO<sub>2</sub> using the method of solution casting. This research work evaluated the influence of BPE and TiO<sub>2</sub> on the physical and structural properties of starch films. The physical properties of the starch films could be significantly altered by the addition of BPE and or TiO<sub>2</sub>. The starch films S/BPE and S/BPE/TiO<sub>2</sub> exhibited higher barrier properties against water vapour as compared to the control films. Incorporation of BPE and TiO<sub>2</sub> could decrease the thickness and moisture content of films. S, S/BPE starch films were transparent and, S/TiO<sub>2</sub> and S/BPE/TiO<sub>2</sub> films were opaque. Control starch films were colourless, whereas S/BPE films have purple colour. Owing to the inclusion of BPE and TiO<sub>2</sub> particles, structural characterization by X-ray diffraction (XRD) and Fourier Transform Infrared Spectroscopy (FTIR) did not show any major changes in polymer structure. Thermogravimetric analysis revealed that the addition of TiO<sub>2</sub> enhanced the thermal stability of starch films to a significant extent. The color of different starch-based films was determined using the CIE Lab scale under different pH conditions and compared with the control. The fabricated (S/BPE and S/BPE/TiO<sub>2</sub>) films exhibited visually perceptible colour changes in the pH range between 1 and 12. Consequently these films could be used as intelligent pH indicators for monitoring the freshness of prawn seafood samples. During the storage of prawn food samples for 6 days, the color of the film changed from light pink to green which is a clear indication of spoilage of food material.

Received 9th July 2020  
Accepted 30th September 2020

DOI: 10.1039/d0ra05986b

rsc.li/rsc-advances

## 1 Introduction

Increased environmental awareness and growing need for the creation of biodegradable polymers have resulted in the advancement of polymer chemistry in a new direction. Rigorous efforts have been taken by researchers to solve the problems generated by the extensive use of plastic materials. Much of the current research is focused on the substitution of petro-based plastics by biodegradable materials with properties comparable to some synthetic polymers.<sup>1,2</sup> In recent decades there has been rapidly growing interest in developing intelligent packaging films as freshness sensors, which is an important aspect for fresh, high quality and safe foods with a longer shelf life, particularly for perishable foods like fish, shrimp, milk, *etc.*<sup>3-6</sup>

Researchers recently developed anthocyanin based material as intelligent or smart materials for food packaging to evaluate

the freshness of a food sample. Novel pH responsive biopolymer films made by immobilising the anthocyanin pigment from natural dyes have received great interest recently.<sup>7-11</sup> The pigment particles immobilised during evaporation and drying process. Immobilisation boosts the orientation of pigments are vertically within the film layer and it is reported that sol gel method is a popular method for immobilisation of pigment. Colorimetric films made from natural pigments and biopolymers are nontoxic safe and biodegradable.

Two main constituents of pH sensitive colorimetric films are a solid base and a pigment to check pH change. Several intelligent pH sensitive biopolymer based films were developed by using different biopolymers like starch<sup>8,10,12-14</sup> bacterial nanocellulose,<sup>8</sup> chitosan,<sup>15</sup> methyl cellulose,<sup>16</sup> polyvinyl alcohol.<sup>15</sup>

Recently natural colour pigments are focused more because they are eco-friendly compared to synthetic dyes. Anthocyanin is one of the best natural pigment and is a water soluble phenolic compound responsible for red, purple, and blue colours in flowers fruits and vegetables. Anthocyanin generally undergo structural changes and exhibit colour variations under different pH conditions. It is an environment friendly pH indicator and

<sup>a</sup>Department of Chemistry, Bishop Moore College, Mavelikara, Kerala, India

<sup>b</sup>Department of Chemistry, CMS College, Kottayam, Kerala, India. E-mail: lapothen@gmail.com; Tel: +91 306 966-5030

<sup>c</sup>IUCNN, Mahatma Gandhi University, Kottayam, Kerala, India



acted as sensor within broad range of pH.<sup>17</sup> Butterfly pea flower (*Clitoria ternatea* L. flowers) are the natural colouring ingredients in tea, food *etc.* The main anthocyanin responsible for the deep blue to purple colour in butterfly pea flower is delphinidin.<sup>18,19</sup>

Titanium dioxide (TiO<sub>2</sub>) is an inert, non-toxic, eco-friendly and inexpensive metal oxide. It exists in three different crystalline forms: rutile (the most stable phase), anatase and brookite. Among these crystalline forms, anatase has the highest photocatalytic activity. TiO<sub>2</sub> can be used to make biopolymer-based packaging films to provide protection against food-borne micro-organisms and allergens in the presence of ultraviolet radiation.<sup>20,21</sup> The anti-microbial activity of TiO<sub>2</sub> is related to reactive oxygen species production.<sup>21</sup> The use of TiO<sub>2</sub> nanoparticles as reinforcement in biopolymer films such as whey protein isolate,<sup>22</sup> wheat starch,<sup>21</sup> soy protein isolate,<sup>23</sup> poly(L-lactic acid)<sup>24</sup> *etc.* have been reported. TiO<sub>2</sub> is generally used in packaging applications as a UV light absorber, and the addition of TiO<sub>2</sub> prevents pathogenic bacteria through antibacterial and antimicrobial effect. The incorporation of TiO<sub>2</sub> nanoparticle also improved the water vapour and oxygen permeability of films.<sup>20</sup>

In this work intelligent packaging films were prepared from potato starch, anthocyanin pigment extracted from butterfly pea flower and TiO<sub>2</sub>. We studied the interesting and promising effect of immobilised anthocyanin and TiO<sub>2</sub> pigment on the properties of starch based films. Influence of BPE extract and TiO<sub>2</sub> on the physical, structural and pH sensitive properties were studied. Finally these intelligent pH sensitive films were employed to monitor the freshness of prawn food sample at refrigeration temperature (4 °C).

## 2 Materials and methods

### 2.1 Materials

Potato starch (S), glycerol, ethyl alcohol, hydrochloric acid, buffer solutions having pH range 1–12, fresh butterfly pea flower collected from local area, TiO<sub>2</sub> (anatase, purity > 98.5%) purchased from KMML Chavara Industry Co., Ltd. All the reagents were of analytical grade. Distilled water was used for all sample preparations.

### 2.2 Extraction of anthocyanin from butterfly pea flower

Anthocyanins were extracted from dried butterfly pea flower by using acid–alcohol mixture.<sup>4,15,17</sup> Dried butterfly pea flower were cut in to small piece and chopped flower were immersed in 1 L of acid–alcohol mixture (ethyl alcohol and water) in the ratio (1 : 3) for 24 h. The extract was filtered and centrifuged at 4000 rpm for 10 minutes. The resultant clear violet coloured supernatant solution was collected and stored in dark place.

### 2.3 Determination of total anthocyanin content (TAC) in BPE by UV

The TAC in BPE was measured *via* the pH differential method using UV-visible spectrophotometer.<sup>6,9,11,25,26</sup> The absorbance of test portion of BPE diluted with pH 1.0 buffer and pH 4.5 buffer at both 520 and 700 nm was measured. In order to get the

absorbance within linear range (between 0.2 and 1.4 absorbance units) determine the appropriate dilution factor. The diluted test portions are read *versus* a blank cell filled with distilled water. Absorbance was measured within 20–50 min of preparation. The anthocyanin content was calculated as cyanidin-3-glucoside (refer to the eqn (1)) with an extinction coefficient of 26 900 and a molecular weight of 484.83 g mol<sup>−1</sup>.

Anthocyanin pigment (cyanidin-3-glucoside equivalents, mg L<sup>−1</sup>)

$$= \frac{A \times \text{MW} \times \text{DF} \times 1000}{\epsilon \times l} \quad (1)$$

where  $A = (A_{520 \text{ nm}} - A_{700 \text{ nm}})_{\text{pH } 1.0} - (A_{520 \text{ nm}} - A_{700 \text{ nm}})_{\text{pH } 4.5}$ , MW (molecular weight) = 484.83 g mol<sup>−1</sup> for cyanidin-3-glucoside, DF = dilution factor,  $l$  = pathlength in cm;  $\epsilon$  = 26 900 molar extinction coefficient, in L & mol<sup>−1</sup> cm<sup>−1</sup>, 1000 = factor for conversion from g to mg.

### 2.4 Colour responses of anthocyanin in BPE to pH changes

Measurement of the colour intensity of anthocyanin extract of BPE was performed on ten pH conditions and the resultant solutions were photographed. Buffer solutions were prepared at a range of pH from 1 to 12 with an aqueous solution of 0.2 M citric acid and 0.2 M disodium hydrogen phosphate and distilled water and then checked by a digital pH meter. To 1 mL of BPE added 9 mL buffer solution and the colour changes were photographed using a digital camera.

### 2.5 Development of starch/extract films by immobilising the anthocyanin pigment

**2.5.1 Preparation of films.** Starch films S, S/BPE, S/TiO<sub>2</sub>, S/BPE/TiO<sub>2</sub> were developed by the method of solution casting.<sup>14,27–31</sup> A quantity of 100 mL of aqueous dispersion containing 5 g of starch and BPE solution having volume corresponding to wt of starch (4% w/w) was then added and 30% glycerol (on a starch dry basis) was added as the plasticiser. The control film was produced without the addition of BPE.

To develop S/TiO<sub>2</sub> (0.5 wt% of TiO<sub>2</sub> on starch matrix), the TiO<sub>2</sub> suspension was ultrasonicated for 1 h and then added slowly to starch solution.<sup>32</sup> To develop S/BPE/TiO<sub>2</sub> (4 wt% of BPE on starch basis) and TiO<sub>2</sub> (0.5 wt% on starch basis) were simultaneously added into starch film forming solution. The solution was mixed well using homogeniser (Ika Ultra-Turrax T 25) and heated to at 85 °C for 10 min.

The film-forming solution was immediately poured into a smooth Teflon sheet. Then, film hydrogels were formed. The hydrogels were dried to films at a temperature of 55 °C for 18 hours. The film was peeled from a Teflon sheet and dried starch films were preserved in a relative humidity (RH = 55%, 25 °C) for further use. The control film was prepared under the same conditions, except that the anthocyanin extract.

### 2.6 Determination of physical properties of films

**2.6.1 Physical appearance and colour.** The films were cut into a rectangle shape and directly placed in a Hunter Lab colorimeter (models 45/0-L), an equipment for colour analysis.



Colour of film samples were evaluated by comparing the values of  $L$ ,  $a$ ,  $b$  to that of control.

Total colour difference ( $\Delta E$ ) and whiteness index (WI) of the films were calculated by the eqn (1) and (2).<sup>4,8,9,14,25</sup>

$$\Delta E = \sqrt{(L^* - L)^2 + (a^* - a)^2 + (b^* - b)^2} \quad (2)$$

$$WI = 100 - \sqrt{(100 - L)^2 + a^2 + b^2} \quad (3)$$

where  $L$ ,  $a$  and  $b$  were the colour indices of control starch  $L^*$ ,  $a^*$  and  $b^*$  were the colour parameters of the BPE incorporated films.

**2.6.2 Film thickness.** The thickness of the films was determined by digital micrometer through randomly selecting ten different positions on each film with the precision of 0.001 mm.

**2.6.3 Moisture content.** The moisture content of film was determined by drying film at 120 °C until constant weight using a moisture analyser (WENSAR Make, Power Supply: AC 220 V/ 50–60 Hz, readability 0.001 g). The analyses were carried out for five samples of each formulation.

**2.6.4 Water vapour permeability (WVP).** WVP of different starch films (S, S/BPE, S/TiO<sub>2</sub> and S/BPE/TiO<sub>2</sub>) were determined by gravimetric method.<sup>33–36</sup> The films were cut in to circle of 2.6 cm diameter and affixed in to the mouth of the cylindrical container cup containing 5 g silica gel (0% RH). Then initial weight of whole device was taken and then placed in a desiccator containing saturated sodium chloride solution (67% RH). The weight of the container cup was weighed and recorded at regular intervals (every 24 h over 5 days). Five measurements were done for each film.

WVP for four starch based films was calculated by the equation:

$$\text{Water vapour permeability} = \frac{W \times X}{t \times A \times \Delta P} \quad (4)$$

where  $W$  is the gain in cup weight (g),  $x$  is film thickness (m),  $t$  is time (s) for the gain in cup weight,  $A$  is the area of film sample

for permeation (m<sup>2</sup>), and  $\Delta P$  is the water vapour pressure difference between the two sides of the film (Pa).

## 2.7 Structural characterization of the films

The surface morphology of the prepared films was observed using an SEM (Carl Zeiss Evo 18 Secondary Electron Microscope With EDS) at room temperature. To obtain SEM images samples were placed on an aluminium base and then covered with gold. FTIR microscopy was conducted on a Perkin Elmer Spectrum 100 FTIR spectrometer within the wave number range of 450–4000 cm<sup>−1</sup> using an attenuated total reflection (ATR) technique. XRD technique was applied to determine the crystalline character of the S, S/BPE, S/TiO<sub>2</sub> and S/BPE/TiO<sub>2</sub> films. Thermal stability of starch films were determined by thermogravimetric analysis (TGA). Samples weighing 10–20 mg were placed in ceramic crucibles, and tests were carried out under nitrogen atmosphere from room temperature (30 °C) up to 500 °C under air atmosphere (30 mL min<sup>−1</sup>) at a heating rate of 10 °C min<sup>−1</sup>.

## 2.8 Colour responses of the films to different pH

Starch films were cut in to small squares (1 cm × 1 cm) and immersed in the buffer solutions having different pH (1–12) for about 5 minutes. Colour changes were photographed.

## 2.9 Application of S/BPE and S/BPE/TiO<sub>2</sub> films for monitoring the freshness of food sample

In order to use the intelligent pH sensitive starch–anthocyanin based films as the freshness sensor, spoilage experiment was carried out by sticking the square shaped (1 cm × 1 cm) films inside the box containing 20 g fresh prawn meat. The box was stored at 4 °C for 6 days. Colour change of pH indicator films were noted and photographed using a digital camera for 6 days.  $\Delta E$  values of the indicator films were assessed in triplicate on days 0, 2, 4 and 6 of storage.

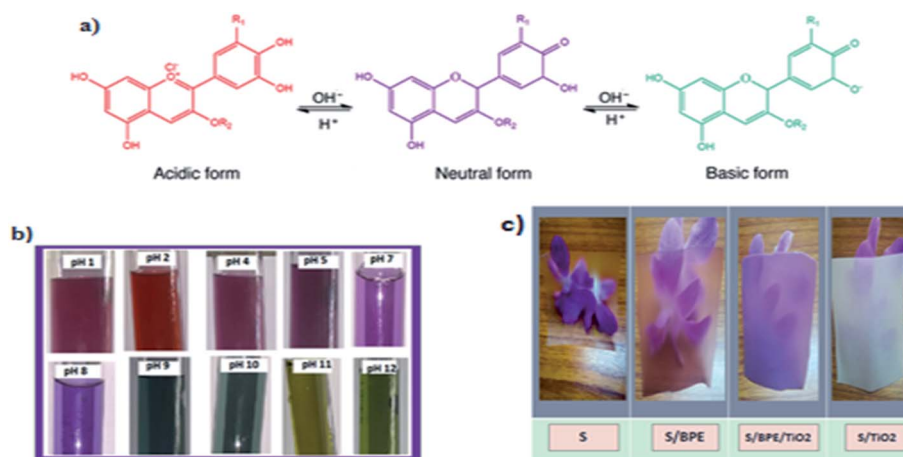


Fig. 1 (a) Chemical diagram of colour-changing anthocyanin pH reaction<sup>37</sup> (b) colour variations of BPE in different buffer solutions (c) photographs of starch films showing the transparency.



**Table 1**  $L^*$ ,  $a^*$ ,  $b^*$ ,  $\Delta E$ , whiteness index (WI), thicknesses, moisture contents, and water vapour permeability of S, S/BPE, S/TiO<sub>2</sub>, S/BPE/TiO<sub>2</sub> films<sup>a</sup>

Films	$L^*$	$a^*$	$b^*$	$\Delta E$	Whiteness index		Thickness (mm)	Moisture content	WVP $\times 10^{-10} \text{ g}^{-1} \text{ s}^{-1} \text{ Pa}^{-1}$
					(WI)				
S	70.18 $\pm$ 0.52 <sup>b</sup>	4.19 $\pm$ 0.41 <sup>c</sup>	−2.51 $\pm$ 0.31 <sup>c</sup>	0	69.8		0.219 $\pm$ 0.009 <sup>a</sup>	15.63 $\pm$ 0.21 <sup>a</sup>	1.49 $\pm$ 0.22 <sup>a,b</sup>
S/BPE	52.25 $\pm$ 0.60 <sup>d</sup>	25.67 $\pm$ 0.31 <sup>a</sup>	2.83 $\pm$ 0.41 <sup>b</sup>	29.12	45.72		0.179 $\pm$ 0.008 <sup>b</sup>	12.78 $\pm$ 0.17 <sup>c</sup>	0.97 $\pm$ 0.057 <sup>b,c</sup>
S/TiO <sub>2</sub>	88.64 $\pm$ 0.14 <sup>a</sup>	1.55 $\pm$ 0.18 <sup>d</sup>	5.58 $\pm$ 0.26 <sup>a</sup>	20.31	87.26		0.182 $\pm$ 0.008 <sup>b</sup>	13.34 $\pm$ 0.27 <sup>b</sup>	0.65 $\pm$ 0.056 <sup>c,d</sup>
S/TiO <sub>2</sub> /BPE	58.46 $\pm$ 0.44 <sup>c</sup>	18.54 $\pm$ 0.35 <sup>b</sup>	−4.8 $\pm$ 0.33 <sup>d</sup>	18.50	54.26		0.184 $\pm$ 0.011 <sup>b</sup>	12.61 $\pm$ 0.34 <sup>c</sup>	0.46 $\pm$ 0.079 <sup>d</sup>

<sup>a</sup> Values are given as mean  $\pm$  SD ( $n = 10$  for film thickness, and  $n = 5$  for moisture content and WVP). Different letters in the same column indicate significantly different ( $p < 0.05$ ).

## 2.10 Statistical analysis

Statistical analysis was conducted by using IBM SPSS Statistics 22.0. The Duncan test and one-way analysis of variance (ANOVA) were used for multiple comparisons by SPSS package. Difference was considered as statistically significant if  $p < 0.05$ .

# 3 Results and discussion

## 3.1 Characterisation of BPE

TAC in BPE was determined as 236.1 mg g<sup>−1</sup> by pH-differential assay. The colour responses of anthocyanins in BPE in different buffer solutions were shown in Fig. 1b. Anthocyanin pigment present in the BPE exhibited colour variations in 10 different pH buffer solutions: bright red at pH 1, purple violet at pH 2–3, purple at pH 4–6 and ocean blue green colour at pH 7–9 and olive green colour at pH 10–12. The colour change of BPE in different buffer solution was attributed to structural changes in anthocyanin pigment.<sup>37</sup>

Thus pH is very important for the colour of anthocyanin. The natural pigment contained in the BPE are red in acid solutions, violet or purple in neutral solutions, and green in alkaline pH. The colour variations of anthocyanin pigment in BPE depend directly on the number of hydroxyl group present in the molecule. Thus pH sensitive films could be used as pH indicators in food industry.<sup>9,19</sup> In this work immobilisation of anthocyanin pigment can be done by incorporating in starch matrix.

## 3.2 Characterisation of S, S/BPE, S/TiO<sub>2</sub> and S/BPE/TiO<sub>2</sub> films

**3.2.1 Physical appearance and colour of starch films.** Colour is an important parameter for intelligent pH sensitive films for the determination of freshness of food samples. As presented in Fig. 1c colour of S/BPE films were significantly different from the control starch films. S, S/BPE starch films were transparent; S/TiO<sub>2</sub> and S/BPE/TiO<sub>2</sub> films were opaque. Control starch films were colourless, whereas S/BPE and S/BPE/TiO<sub>2</sub> films have grape purple colour. The grape purple colour of S/BPE film was due to the intrinsic colour of BPE. Starch/BPE films shows higher ' $a^*$ ' value than control films ascribed to the grape purple colour of the films. The total colour difference ( $\Delta E$ ) of starch films increases with the addition of BPE indicating that S/BPE and S/BPE/TiO<sub>2</sub> are more coloured.<sup>25,38</sup> The value of WI increased from 69.8 to 87.26 revealing the deepness in white colour by the addition of TiO<sub>2</sub> to starch matrix. The white colour of S/TiO<sub>2</sub> film could be caused by the aggregates of

TiO<sub>2</sub> particles.  $L^*$  and whiteness index (WI) values of starch films decreased by the addition of BPE. Similar results were observed when micro particles of blackberry pulp were added to arrowroot starch.<sup>39</sup>

**3.2.2 Film thickness.** As presented in the Table 1 thickness of films varied from 0.219 to 0.179 mm. Thickness is an important parameter affecting the opacity, water vapour permeability and its usage as freshness sensor. By the incorporation of BPE and TiO<sub>2</sub>, there occurs slight change in the value of film thickness, which may be due to the good dispersion of BPE and TiO<sub>2</sub> particles in the starch matrix. Strong intermolecular interactions between starch, BPE, and TiO<sub>2</sub> reduces the thickness of films.<sup>38</sup>

**3.2.3 Moisture content.** The moisture content of different starch films are shown in the Table 1. Moisture content value of starch/BPE films is lower than that of control. Interaction between hydroxyl group of starch and anthocyanins present in BPE lowered the number of free hydroxyl group to intermingle with moisture.<sup>25</sup> The voids present in the starch matrix is decreased by incorporating TiO<sub>2</sub>, which consecutively lowered the moisture content in S/TiO<sub>2</sub> films.<sup>32</sup>

**3.2.4 Water vapour permeability.** The results of Water Vapour Permeability (WVP) of different starch based shown in the Table 1 indicate that the addition of BPE and TiO<sub>2</sub> has a key role in the reduction of WVP of starch films. The WVP values of control starch films was  $1.49 \pm 0.22 \times 10^{-10} \text{ g m}^{-1} \text{ s}^{-1} \text{ Pa}^{-1}$  that close to other studies reported in the literature.<sup>21</sup> The lower

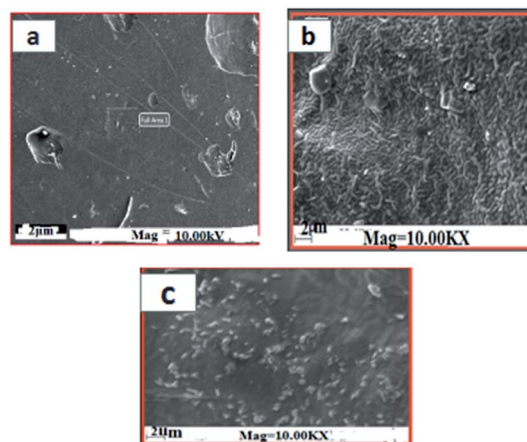


**Fig. 2** Scanning electron microscope micrographs of (a) S (b) S/BPE and (c) S/BPE/TiO<sub>2</sub> starch based films.





WVP values of BPE films ( $0.97 \pm 0.057 \times 10^{-10} \text{ g m}^{-1} \text{ s}^{-1} \text{ Pa}^{-1}$  for S/BPE and  $0.46 \pm 0.079 \times 10^{-10} \text{ g m}^{-1} \text{ s}^{-1} \text{ Pa}^{-1}$  for S/BPE/TiO<sub>2</sub>) may be due to hydrogen and covalent interaction between starch matrix and hydroxyl group anthocyanin pigment which reduces the availability of free hydroxyl group leading to a decrease in hydrophilicity. Similar findings were observed in the literature.<sup>40</sup> TiO<sub>2</sub> incorporated S/TiO<sub>2</sub> and S/BPE/TiO<sub>2</sub> films have WVP values of  $0.65 \pm 0.056 \times 10^{-10} \text{ g m}^{-1} \text{ s}^{-1} \text{ Pa}^{-1}$  and  $0.46 \pm 0.079 \times 10^{-10} \text{ g m}^{-1} \text{ s}^{-1} \text{ Pa}^{-1}$  respectively. The lower values of WVP for these films were due to the blocking water vapour paths in the film network by TiO<sub>2</sub> nanoparticles. TiO<sub>2</sub> particles also interact with hydroxyl group of starch with formation of dense networks and reduced available hydrophilic groups for the sorption of water vapour.<sup>32,38</sup> The results revealed that BPE and TiO<sub>2</sub> particle had a key role in reducing the WVP values of starch films.

### 3.3 Structural characterization of the starch films

**3.3.1 SEM.** The surface morphology of S, S/BPE and S/BPE/TiO<sub>2</sub> was probed by SEM (Fig. 2). The surface morphology of the starch film appeared almost homogeneous. As shown in the figure, surface of S/BPE films was found to be rough indicating that anthocyanin extract was homogeneously mixed and there exist strong interaction between starch and BPE. Addition of phenolic compounds like anthocyanin promote the formation of hydrogen bonds with the starch matrix.<sup>11</sup> Polymer chains were uniformly blended. But S/BPE/TiO<sub>2</sub> films showed rough surface structures with evenly distributed TiO<sub>2</sub> particles. SEM results showed that the TiO<sub>2</sub> particles were homogeneously distributed through the whole film surfaces. The presence of TiO<sub>2</sub> particles was clearly visible in the SEM micrographs.

**3.3.2 FTIR analysis.** The FT-IR spectra of the different starch based films are shown in Fig. 3. FTIR spectra of starch film had typical characteristic peaks at 918, 1000 and 1153 cm<sup>-1</sup> (CO stretching), 1424 cm<sup>-1</sup> (glycerol), 1642 cm<sup>-1</sup> (bound water), 3258 cm<sup>-1</sup> (O-H groups), 2927 cm<sup>-1</sup> (C-H stretching). The same results were observed in the literature.<sup>41,42</sup> The interaction of

starch and BPE in S/BPE films was reflected in the spectrum. The absorption band at 1610 cm<sup>-1</sup> can be attributed to the stretching COO vibration and reveals the presence of an ester bond of carbonyl or carboxylic acid. The band at 1338 cm<sup>-1</sup> corresponds to the O-H in plane deformation in polyphenols.<sup>18</sup> The intense absorption bands at 3258, 3268, 3276 cm<sup>-1</sup> and were attributed to O-H stretching vibrations.<sup>43</sup> Peak at 1416 cm<sup>-1</sup> shows stretching vibrations of Ti-O-Ti. Moreover, there are no significant variations in terms of intensity or band shifting by the addition of both anthocyanin extract and TiO<sub>2</sub> particles.

**3.3.3 XRD pattern of starch films.** X-ray diffraction analysis was performed to reveal the crystalline character of different starch films. The XRD patterns of S, S/BPE, S/TiO<sub>2</sub> and S/BPE/TiO<sub>2</sub> films were shown in Fig. 4. The intermolecular force of attraction between starch, glycerol, BPE, and TiO<sub>2</sub> in different starch films can be studied with the help of XRD. Control starch films show diffraction peaks at 2θ of 17.3°, 19.5°, 22.5° and 25.8° with weak intensity.<sup>44,45</sup>

No sharp diffraction peaks were observed corresponding to the anthocyanin pigment and S/BPE films showed amorphous pattern similar to that of starch. The diffraction peak intensities of BPE incorporated films were stronger than other films. This may attributed to the formation of hydrogen bonding between starch and anthocyanin pigment.<sup>25</sup> A weak diffraction pattern was observed for S/BPE/TiO<sub>2</sub> film compared to S/TiO<sub>2</sub> film, which could be attributed to the intermolecular interactions among S, TiO<sub>2</sub> and BPE.<sup>38,46</sup>

**3.3.4 Thermogravimetric analysis.** Thermogravimetric analysis of different starch based films were carried out to evaluate the thermal stabilities and degradation profiles of starch films. TG curve of starch based films are displayed in Fig. 5. The reported results available from the literature suggested that TGA curve of starch thermoplastic starch films exhibited a three-step thermal degradation pattern.<sup>29</sup> First weight loss from 40 °C was associated with the evaporation of water and glycerol. The second stage of thermal degradation started at 254 °C, 238 °C, 280 °C, and 271 °C for S, S/BPE, S/TiO<sub>2</sub> and S/BPE/TiO<sub>2</sub> films respectively.

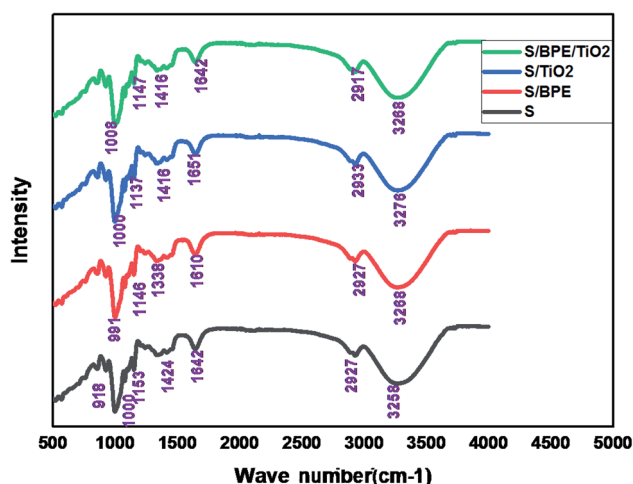


Fig. 3 FTIR spectra of S, S/BPE, S/TiO<sub>2</sub> and S/BPE/TiO<sub>2</sub> films.

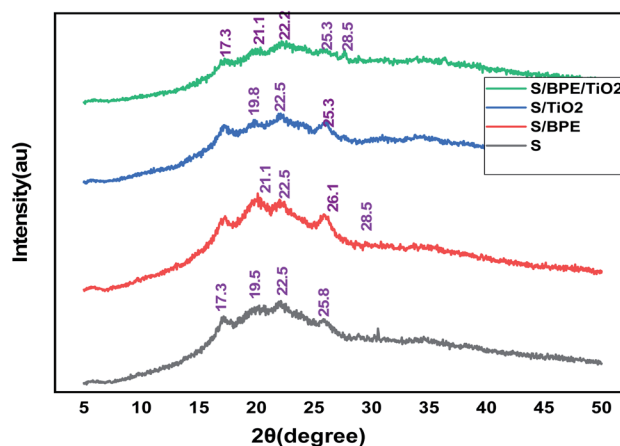


Fig. 4 XRD patterns for the control starch film, S/BPE, S/TiO<sub>2</sub> and S/BPE/TiO<sub>2</sub> films.



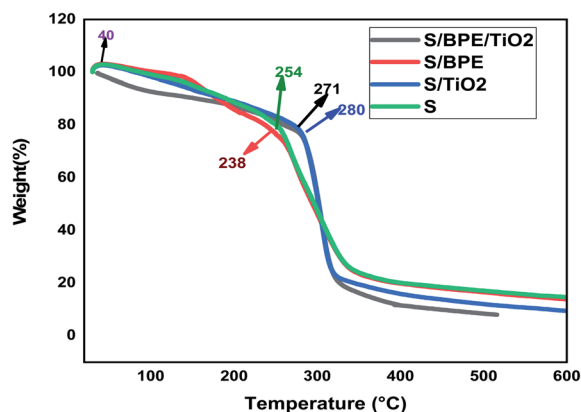


Fig. 5 TG curves of S, S/BPE, S/TiO<sub>2</sub> and S/BPE/TiO<sub>2</sub> films.

The main weight loss occurred at this stage which was ascribed to the decomposition of starch films.<sup>9</sup> The results revealed that the addition of BPE to starch matrix reduced the thermal stability of starch films. But the addition of TiO<sub>2</sub> enhanced the thermal stability of starch films to a significant extent. The third stage in the thermogram ascribed to the complete degradation of polymer.

### 3.4 Colour responses of the films to different pH

Anthocyanin incorporated starch films should exhibit colour change with pH and could be used as intelligent pH indicator films to monitor the freshness of the packaged food. S/BPE and S/TiO<sub>2</sub>/BPE films both showed remarkable colour changes in the range of pH 1–12. For the determination of correlation of pH and colour change, pH indicator films with BPE were immersed in buffer solutions containing different pH values within the range 1–12. Similar colour changes were observed as per previous work, such as chitosan–purple sweet potato extract films, chitosan – black plum peel extract films, starch–blueberry residue films, chitosan–silver – purple corn extract films.<sup>7,14,46</sup>

For pH values (1 to 4) colour of the S/BPE films varies from reddish pink to purple. The appearance of red and pink colour

may be due to the presence of the flavylium cation.<sup>7,46</sup> When the film was in contact with buffer solution with pH range 5–7, S/BPE films showed a violet colour. In basic buffer solution the film showed entirely different colour as compared to colour range in acidic medium. In basic buffer solution having pH 8–10 film, the colour of the film changed to blue. At pH 10 to 12 the S/BPE films appeared a bright greenish blue colour. Colour of the films varies from bright purple – blue – green from pH 1 to pH 12. This same colour spectrum was reported in ref. 15 who found that an anthocyanin based pH indicator films exhibit same colour change in acidic–neutral–basic buffer solutions. S/BPE/TiO<sub>2</sub> also exhibited almost similar colour pattern in different pH conditions. At pH 1 films shows an excellent bright red colour compared to S/BPE films. The presence of TiO<sub>2</sub> increases the brightness of different colours. Our results suggested that both S/BPE and S/BPE/TiO<sub>2</sub> films are excellent pH indicators for monitoring the freshness of packaged food samples.

The value of colour parameters  $L^*$ ,  $a^*$  and  $b^*$  obtained by using the Hunter Lab colorimeter is given in the Table 2 confirmed the results shown in Fig. 6. Table 2 summarizes the colour parameters  $L^*a^*b^*$  values in CIELab\* scale, colour difference ( $\Delta E$ ) and whiteness indices (WI) for the S/BPE films after being immersed in different buffer solution. Values of total colour difference ( $\Delta E$ ) greater than 3 can be considered visually perceptible to the human eye. In the present work, according to Table 2,  $\Delta E$  were above 3.00. Films at alkaline pH showed highest  $\Delta E$  values, which show a marked visual colour difference. Both the BPE incorporated samples (S/BPE and S/BPE/TiO<sub>2</sub> starch films) exhibited visually perceptible differences.<sup>47</sup>

In acidic region  $L^*$  value is maximum for films at pH = 1, which indicates that at this pH film more intense red colour.<sup>17</sup> In basic region  $L^*$  value is maximum at pH = 12 and pH = 10 for S/BPE and S/BPE/TiO<sub>2</sub> respectively, reveals that in alkaline medium intense green colour is exhibited by these films at this pH. The S/BPE films exhibited negative  $b^*$  (blue to yellow) gradually increased from  $-2.55 \pm 0.24$  to  $-26.52 \pm 0.37$  corresponding to the colour change from red to blue. Almost similar

Table 2 Colourimetric parameters in CIELab\* scale, of S/BPE starch films after being immersed in different pH values (1–12) in comparison with the  $L^*a^*b^*$  values films at pH 7<sup>a</sup>

pH	S/BPE				S/BPE/TiO <sub>2</sub>			
	$L^*$	$a^*$	$b^*$	$\Delta E$	$L^*$	$a^*$	$b^*$	$\Delta E$
1	44.21 ± 0.44 <sup>b</sup>	21.68 ± 0.27 <sup>c</sup>	-2.55 ± 0.24 <sup>a</sup>	24.53	56.40 ± 0.24 <sup>a</sup>	38.55 ± 0.36 <sup>a</sup>	15.71 ± 0.26 <sup>f</sup>	16.70
2	40.87 ± 0.16 <sup>c</sup>	25.48 ± 0.36 <sup>b</sup>	-2.46 ± 0.30 <sup>a</sup>	29.07	53.69 ± 0.21 <sup>b</sup>	25.53 ± 0.35 <sup>d</sup>	-8.56 ± 0.28 <sup>d</sup>	20.89
4	39.08 ± 0.25 <sup>g</sup>	31.53 ± 0.23 <sup>a</sup>	-5.51 ± 0.50 <sup>b</sup>	32.59	46.72 ± 0.60 <sup>c</sup>	25.45 ± 0.42 <sup>d</sup>	20.60 ± 0.38 <sup>g</sup>	10.30
5	42.66 ± 0.29 <sup>c</sup>	21.67 ± 0.22 <sup>c</sup>	20.39 ± 0.25 <sup>e</sup>	7.62	52.35 ± 0.33 <sup>d</sup>	30.66 ± 0.32 <sup>b</sup>	27.41 ± 0.36 <sup>h</sup>	18.37
7	40.48 ± 0.24 <sup>c</sup>	25.64 ± 0.29 <sup>b</sup>	26.52 ± 0.37 <sup>f</sup>	0	45.34 ± 0.36 <sup>f</sup>	27.15 ± 0.15 <sup>c</sup>	10.53 ± 0.28 <sup>e</sup>	0
8	37.51 ± 0.38 <sup>h</sup>	16.48 ± 0.36 <sup>d</sup>	15.35 ± 0.21 <sup>d</sup>	14.75	41.89 ± 0.61 <sup>g</sup>	25.14 ± 0.56 <sup>f</sup>	-3.37 ± 0.59 <sup>b</sup>	52.88
9	41.44 ± 0.41 <sup>d</sup>	15.43 ± 0.59 <sup>d</sup>	-6.61 ± 0.43 <sup>c</sup>	22.39	45.64 ± 0.32 <sup>f</sup>	30.52 ± 0.36 <sup>g</sup>	0.51 ± 0.32 <sup>a</sup>	58.71
10	39.9 ± 0.21 <sup>f</sup>	10.35 ± 0.21 <sup>f</sup>	20.50 ± 0.32 <sup>e</sup>	16.44	52.95 ± 0.41 <sup>c</sup>	35.62 ± 0.39 <sup>i</sup>	-7.70 ± 0.22 <sup>c</sup>	62.40
11	37.62 ± 0.34 <sup>h</sup>	19.42 ± 0.30 <sup>g</sup>	-5.39 ± 0.34 <sup>b</sup>	49.85	37.62 ± 0.34 <sup>h</sup>	34.73 ± 0.76 <sup>h</sup>	-3.77 ± 0.44 <sup>b</sup>	62.72
12	45.14 ± 0.55 <sup>a</sup>	30.58 ± 0.35 <sup>h</sup>	-2.75 ± 0.33 <sup>a</sup>	61.29	40.59 ± 0.37 <sup>h</sup>	20.29 ± 0.62 <sup>e</sup>	10.03 ± 0.37 <sup>c</sup>	51.92

<sup>a</sup> Values are given as  $\pm$  SD ( $n = 5$ ). Different letters in the same column indicates the values are significantly different ( $p < 0.05$ ).



Films	pH 1	pH 2	pH 4	pH 5	pH 7	pH 8	pH 9	pH 10	pH 11	pH 12
S/BPE										
S/TiO <sub>2</sub> /BPE										

Fig. 6 Visual aspect colour of the S/BPE and S/BPE/TiO<sub>2</sub> starch pH indicator films with butterfly pea extract after immersion in buffer solutions having different pH values (1–12).

variations in  $b$  values were also observed in the case of S/BPE/TiO<sub>2</sub> films. The changes in the  $-b^*$  values were in good agreement with the observed colour changes of the film. The colour parameter  $a^*$  (red to green) from Table 2, with a maximum value of  $38.55 \pm 0.36$  (pH1 for S/BPE/TiO<sub>2</sub>) agreed well with intense red colour of film. Among the two starch pH indicator films (S/BPE and S/BPE/TiO<sub>2</sub>), S/BPE/TiO<sub>2</sub> was brightest confirmed by highest  $L^*$  and WI values. This increase in whiteness may attribute to the white colour of TiO<sub>2</sub> particles.

### 3.5 Application of pH indicator films as the freshness indicator

We used both S/BPE and S/BPE/TiO<sub>2</sub> film as the freshness indicator to monitor the freshness of prawn sample. The photocatalytic self-cleaning property of TiO<sub>2</sub> made the S/BPE/TiO<sub>2</sub> film as a better suitable intelligent films for freshness monitoring. Microbial activity is the main reason for spoilage of prawn. High levels of total volatile basic nitrogen such as dimethylammonium, trimethylamine and ammonia were produced by the microbiological contamination of spoiled food. Since the film was stuck inside the cap of box there exist no direct contact between films and prawn sample. Initial pH of

the fresh samples was 6.58. During the spoilage, pH of the sample increased due to the proteins hydrolysis followed by the formation of volatile compounds.<sup>8,9</sup> The films will respond to the volatile basic compound evolved from the sample during the spoilage. The evolution of basic compounds resulted in the increase in pH near the atmosphere of films within the closed container. As pH gradually increased, the colour of S/BPE and S/BPE/TiO<sub>2</sub> films changed from pink to green and visually demonstrated in the Fig. 7. Similar results was also reported by other researchers.<sup>48</sup>

Colour parameters  $L^*a^*b^*$  values, and  $\Delta E$  of freshness indicator films at different time intervals (0, 2, 4, 6 days) were summarized in the Table 3. Both the films showed an obvious colour change as storage time is prolonged. The colour of the film changed to green from light pink. For S/BPE and S/BPE/TiO<sub>2</sub> the value of  $a^*$  changes from  $25.55 \pm 0.37$  to  $-30.69 \pm 0.28$  and  $16.47 \pm 0.47$  to  $-33.90 \pm 0.89$  respectively. The value of  $\Delta E$  indicates that there occurs appreciable colour change during the storage of prawn food sample for 6 days which is clear indication of spoilage of food material. S/BPE and S/BPE/TiO<sub>2</sub> pH indicator films can thus acted as non-destructive detector for spoilage of food material by changing its colour from light pink(fresh stage) to intense green(beginning of spoilage). This

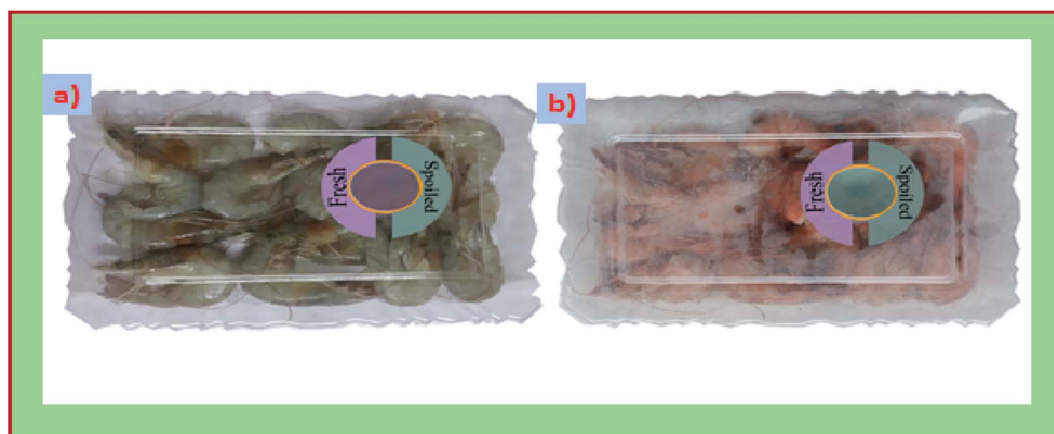


Fig. 7 Color changes in the intelligent pH indicator starch based films (S/BPE/TiO<sub>2</sub>) attached to packages of prawn seafood sample (a) immediately after packaging (b) after 6 days of storage at 4 °C.



**Table 3** Colour responses of S/BPE and S/BPE/TiO<sub>2</sub> films at different time intervals (0, 2, 4, 6 days) for prawn freshness monitoring<sup>a</sup>

Days	L*	a*	b*	ΔE
<b>S/BPE</b>				
0	50.90 ± 0.54 <sup>c</sup>	25.55 ± 0.37 <sup>a</sup>	−1.79 ± 0.37 <sup>b</sup>	
2	58.82 ± 0.60 <sup>a</sup>	21.46 ± 0.91 <sup>b</sup>	−7.00 ± 0.37 <sup>c</sup>	24.83
4	52.10 ± 0.67 <sup>b</sup>	10.60 ± 0.52 <sup>c</sup>	−20.89 ± 0.37 <sup>d</sup>	20.44
6	41.29 ± 0.71 <sup>d</sup>	−30.69 ± 0.28 <sup>d</sup>	4.93 ± 0.37 <sup>a</sup>	57.45
<b>S/BPE/TiO<sub>2</sub></b>				
0	54.94 ± 0.37 <sup>d</sup>	16.47 ± 0.47 <sup>a</sup>	−7.04 ± 0.51 <sup>c</sup>	
2	60.88 ± 0.39 <sup>c</sup>	13.05 ± 0.84 <sup>b</sup>	−12.16 ± 0.98 <sup>d</sup>	8.55
4	62.31 ± 0.46 <sup>b</sup>	8.96 ± 0.49 <sup>c</sup>	−2.43 ± 0.49 <sup>a</sup>	11.48
6	65.49 ± 0.65 <sup>a</sup>	−33.90 ± 0.89 <sup>d</sup>	−5.08 ± 0.70 <sup>b</sup>	51.48

<sup>a</sup> Values are given as ± SD. Different letters in the same column indicates the values are significantly different ( $p < 0.05$ ).

colour change can be easily distinguished by direct observation. Ezati *et al.*<sup>8</sup> prepared pH sensitive indicator film based on starch-cellulose and alizarin dye to monitor the freshness of rainbow trout fillet at 4 °C and analysed the color changes. These results indicated that natural pigment (anthocyanin extracted from butterfly pea flower) incorporated starch films are excellent eco-friendly and safe indicator for monitoring the freshness of food sample.

## 4 Conclusion

In this work intelligent pH sensitive starch based films were successfully developed by incorporating anthocyanin extracted from butterfly pea flower and TiO<sub>2</sub>. It was observed that the addition of BPE and TiO<sub>2</sub> could greatly alter the physical properties of the films (colour, transparency, thickness, moisture content, water vapour permeability and thermal stability). SEM, FTIR XRD and TG analysis confirmed the presence of intermolecular interactions among S, BPE and TiO<sub>2</sub>. Starch based films (S/BPE and S/BPE/TiO<sub>2</sub>) exhibited an appreciable colour change in different buffer solutions having pH (1–12). The application trial for the usage of the film S/BPE/TiO<sub>2</sub> as freshness monitor revealed that there occurs appreciable colour change from light pink (fresh stage) to intense green (beginning of spoilage). We could distinguish the colour with naked eye. This colour change is attributed to increase in pH of the food sample by evolution of basic compounds during spoilage. Hence, these intelligent films can be used as safe and eco-friendly pH indicator films for monitoring the freshness of seafood sample.

## Conflicts of interest

There are no conflicts to declare.

## References

- 1 F. Zia, K. M. Zia, M. Zuber, S. Kamal and N. Aslam, *Carbohydr. Polym.*, 2016, **134**, 784–798.

- 2 a. Orue, M. a. Corcuera, C. Pena, A. Eceiza and A. Arbelaiz, *J. Thermoplast. Compos. Mater.*, 2014, **29**, 817–832.
- 3 B. Kuswandi, *Freshness Sensors for Food Packaging*, Elsevier, 2017.
- 4 H. Chen, M. Zhang, B. Bhandari and C. Yang, *Food Hydrocolloids*, 2020, **100**, 105438.
- 5 S. Mohammadalinejad, H. Almasi and M. Moradi, *Food Control*, 2020, **113**, 107169.
- 6 M. M. Goodarzi, M. Moradi, H. Tajik, M. Forough, P. Ezati and B. Kuswandi, *Int. J. Biol. Macromol.*, 2020, **153**, 240–247.
- 7 H. Yong, X. Wang, R. Bai, Z. Miao, X. Zhang and J. Liu, *Food Hydrocolloids*, 2019, **90**, 216–224.
- 8 P. Ezati, H. Tajik, M. Moradi and R. Molaei, *Int. J. Biol. Macromol.*, 2019, **132**, 157–165.
- 9 D. Yun, H. Cai, Y. Liu, L. Xiao, J. Song and J. Liu, *RSC Adv.*, 2019, **9**, 30905–30916.
- 10 D. Yun, H. Cai, Y. Liu, L. Xiao, J. Song and J. Liu, *RSC Adv.*, 2019, 30905–30916.
- 11 X. Zhai, Z. Li, J. Zhang, J. Shi, X. Zou, X. Huang, D. Zhang, Y. Sun, Z. Yang, M. Holmes, Y. Gong and M. Povey, *J. Agric. Food Chem.*, 2018, **66**, 12836–12846.
- 12 Z. Xiaodong, J. Shi, Z. Xiaobo, W. Sheng, J. Caiping, Z. Junjun, H. Xiaowei, W. Zhang and H. Mel, *Food Hydrocolloids*, 2017, **69**, 308–317.
- 13 I. Choi, J. Young, M. Lacroix and J. Han, *Food Chem.*, 2017, **218**, 122–128.
- 14 C. L. Luchese, V. F. Abdalla, J. C. Spada and I. C. Tessaro, *Food Hydrocolloids*, 2018, **82**, 209–218.
- 15 Q. De Arruda, R. Stefani, V. Aniceto, P. Jr and I. Nat, *Food Hydrocolloids*, 2015, **43**, 180–188.
- 16 A. Nopwinyuwong, S. Trevanich and P. Suppakul, *Talanta*, 2010, **81**, 1126–1132.
- 17 T. Vo and T. Dang, *Polymers*, 2020, **11**, 107169.
- 18 A. Mehmood, M. Ishaq, L. Zhao, S. Yaqoob, B. Safdar, M. Nadeem, M. Munir and C. Wang, *Ultrason. Sonochem.*, 2019, **51**, 12–19.
- 19 S. A. T. Lakshan, N. Y. Jayanath, W. P. K. M. Abeysekera and W. K. S. M. Abeysekera, *Evid.-Based Complementary Altern. Med.*, 2019, 1–13.
- 20 E. Arezoo, E. Mohammadreza, M. Maryam and M. N. Abdorreza, *Int. J. Biol. Macromol.*, 2020, **157**, 743–751.
- 21 V. Goudarzi, I. Shahabi-ghahfarrokhi and A. Babaei-qazvini, *Int. J. Biol. Macromol.*, 2017, **95**, 306–313.
- 22 Y. Li, Y. Jiang, F. Liu, F. Ren, G. Zhao and X. Leng, *Food Hydrocolloids*, 2011, **25**, 1098–1104.
- 23 Z. Wang, N. Zhang, H. Y. Wang, S. Y. Sui, X. X. Sun and Z. S. Ma, *LWT-Food Sci. Technol.*, 2014, **57**, 548–555.
- 24 N. Nakayama and T. Hayashi, *Polym. Degrad. Stab.*, 2007, **92**, 1255–1264.
- 25 Y. Qin, Y. Liu, H. Yong, J. Liu, X. Zhang and J. Liu, *Int. J. Biol. Macromol.*, 2019, **134**, 80–90.
- 26 T. N. Pham, D. C. Nguyen, T. D. Lam, P. Van Thinh and X. Tien, *Mater. Sci. Eng.*, 2019, **542**, 12032.
- 27 P. Kanmani and J.-W. Rhim, *Carbohydr. Polym.*, 2014, **106**, 190–199.





- 28 N. El Miri, K. Abdelouahdi, A. Barakat, M. Zahouily, A. Fihri, A. Solhy and M. El Achaby, *Carbohydr. Polym.*, 2015, **129**, 156–167.
- 29 Y. Qin, S. Zhang, J. Yu, J. Yang, L. Xiong and Q. Sun, *Carbohydr. Polym.*, 2016, **147**, 372–378.
- 30 H. Wang, L. Wang, S. Ye and X. Song, *Food Hydrocolloids*, 2019, **88**, 92–100.
- 31 S. H. Othman, N. R. A. Kechik, R. A. Shapi, R. A. Talib and I. S. M. A. Tawakkal, *J. Nanomater.*, 2019, 1–12.
- 32 V. Goudarzi, I. Shahabi-ghahfarrokhi and A. Babaei-ghazvini, *Int. J. Biol. Macromol.*, 2017, **95**, 306–313.
- 33 M. Sapper, P. Talens and A. Chiralt, *Int. J. Polym. Sci.*, 2019, 1–9.
- 34 J. L. Guimarães, F. Wypych, C. K. Saul, L. P. Ramos and K. G. Satyanarayana, *Carbohydr. Polym.*, 2010, **80**, 130–138.
- 35 Y. Qin, S. Zhang, J. Yu, J. Yang, L. Xiong and Q. Sun, *Carbohydr. Polym.*, 2016, **147**, 372–378.
- 36 K. González, A. Retegi, A. González, A. Eceiza and N. Gabilondo, *Carbohydr. Polym.*, 2015, **117**, 83–90.
- 37 V. Kan, E. Vargo, N. Machover, H. Ishii, S. Pan, W. Chen and Y. Kakehi, *Proc. 2017 CHI Conf. Hum. factors Comput. Syst.*, 2017, pp. 989–1000.
- 38 X. Zhang, Y. Liu, H. Yong, Y. Qin, J. Liu and J. Liu, *Food Hydrocolloids*, 2019, **94**, 80–92.
- 39 G. F. Nogueira, F. M. Fakhouri, J. I. Velasco and R. A. de Oliveira, *Polymers*, 2019, **11**, 1382.
- 40 Y. C. Wei, C. H. Cheng, Y. C. Ho, M. L. Tsai and F. L. Mi, *Food Hydrocolloids*, 2017, **69**, 491–502.
- 41 O. Lopez, M. a. Garcia, M. a. Villar, a. Gentili, M. S. Rodriguez and L. Albertengo, *LWT–Food Sci. Technol.*, 2014, **57**, 106–115.
- 42 G. Abera, B. Woldeyes, H. D. Demash and G. Miyake, *Int. J. Biol. Macromol.*, 2020, **155**, 581–587.
- 43 A. Alshehri and A. Malik, *RSC Adv.*, 2017, **7**, 25149–25159.
- 44 A. Ali, Y. Chen, H. Liu, L. Yu, Z. Baloch, S. Khalid, J. Zhu and L. Chen, *Int. J. Biol. Macromol.*, 2019, **129**, 1120–1126.
- 45 J. Chen, Z. Long, S. Wang, Y. Meng, G. Zhang and S. Nie, *Int. J. Biol. Macromol.*, 2019, **139**, 367–376.
- 46 Y. Qin, Y. Liu, L. Yuan, H. Yong and J. Liu, *Food Hydrocolloids*, 2019, **96**, 102–111.
- 47 R. Andretta, C. L. Luchese, I. C. Tessaro and J. C. Spada, *Food Hydrocolloids*, 2019, **93**, 317–324.
- 48 S. Kang, H. Wang, M. Guo, L. Zhang, M. Chen, S. Jiang, X. Li and S. Jiang, *J. Agric. Food Chem.*, 2018, **66**, 13268–13276.

